



# The dependency of the $\delta^{18}\text{O}$ discrepancy between ice cores and model simulations on the spatial model resolution

Marcus Breil<sup>1</sup>, Emanuel Christner<sup>1</sup>, Alexandre Cauquoin<sup>2</sup>, Martin Werner<sup>2</sup>, Gerd Schädler<sup>1</sup>

<sup>1</sup>Institute of Meteorology and Climate Research, Karlsruhe Institute of Technology, Eggenstein-Leopoldshafen, Germany

5 <sup>2</sup>Alfred Wegener Institute, Helmholtz Centre for Polar and Marine Sciences, Bremerhaven, Germany

*Correspondence to:* Marcus Breil (Marcus.breil@kit.edu)

**Abstract.** In this study, regional climate simulations under present-day and mid-Holocene conditions are performed with an isotope-enabled RCM for Greenland. The capability of the applied isotope-enabled Regional Climate Model (RCM), COSMO\_iso, to reproduce observed isotopic ratios in Greenland for these two periods is investigated by downscaling global  
10 ECHAM5-wiso present-day and MPI-ESM-wiso mid-Holocene simulations for the Arctic region. The RCM model results are subsequently compared to measured  $\delta^{18}\text{O}$  ratios from snow pit samples and ice cores. To our knowledge, this is the first time that a mid-Holocene isotope-enabled RCM simulation is performed for the Arctic region.

Under present-day conditions, a downscaling with COSMO\_iso to a spatial resolution of 50 km improves the agreement with the measured  $\delta^{18}\text{O}$  ratios for 11 of 16 observational data sets. A further increase in the spatial resolution to 7 km yield only  
15 improvements for the coastal areas with its complex terrain. Furthermore, by investigating the  $\delta^{18}\text{O}$  ratios in all COSMO\_iso grid boxes located within the corresponding ECHAM5-wiso grid box, the observed isotopic ratios can be classified as a possible local  $\delta^{18}\text{O}$  ratio within the spatial uncertainties, derived by the regional downscaling approach. For the mid-Holocene, a fully coupled MPI-ESM-wiso time slice simulation is downscaled with COSMO\_iso to a spatial resolution of 50 km. The model performance of MPI-ESM-wiso in the mid-Holocene is already on a high level for Greenland and a downscaling with  
20 COSMO\_iso does not further improve the model-data agreement. But again, the range of the COSMO\_iso\_50km  $\delta^{18}\text{O}$  variability in the corresponding MPI-ESM-wiso grid boxes around each station is consistent with the observed  $\delta^{18}\text{O}$  values. The correct  $\delta^{18}\text{O}$  ratios are consequently already included but hidden in the MPI-ESM-wiso results, which just need to be extracted by a refinement with an RCM. Thus, an isotope-enabled GCM-RCM model chain with realistically implemented fractionating processes, constitutes a useful supplement to reconstruct regional paleo-climate conditions during the mid-  
25 Holocene in Greenland. Such model chains might also be applied to reveal the full potential of GCMs in regions and climate periods, in which large deviations to observed isotope ratios are simulated.

## 1 Introduction

Stable isotopes of water ( $\text{HD}^{16}\text{O}$  and  $\text{H}_2^{18}\text{O}$ ) are fractionated during any phase transition. This fractionating process depends on temperature (Dansgaard, 1953; Craig and Gordon, 1965; Jouzel and Merlivat, 1984), so that water isotopic ratios (expressed



30 here in the usual  $\delta$  notation,  $\delta D$  and  $\delta^{18}O$  with respect to the Vienna Standard Mean Ocean Water V-SMOW) reflect the atmospheric conditions under which the fractionating process took place (Dansgaard, 1964; Merlivat and Jouzel, 1979; Gat, 1996). This process is generally utilized to reconstruct paleo-climate conditions like past changes of temperature, out of isotopic ratios stored in climate archives (Dansgaard et al., 1969; Masson-Delmotte et al., 2005; Jouzel, 2013).

In Arctic regions like Greenland, ice cores constitute an exceptional climate archive. Over thousands of years, accumulated  
35 snow was solidified to ice, preserving at some locations the water isotopic ratios since the last interglacial period. Climate reconstructions based on these ice cores show that the climate conditions changed considerably in Greenland during the Holocene (here defined as the period between present-day and 12 ka; Marcott et al., 2013). Temperature was steadily rising during the early Holocene, until the Holocene Thermal Maximum was reached in the mid-Holocene (6 ka). Since then, temperatures were steadily decreasing until the late Holocene (Marcott et al., 2013; Moossen et al., 2015). In this context, the  
40 mid-Holocene is a period of particular interest, as by that time an Arctic warming took place due to orbital forcing variations and their related feedbacks on large-scale climate variations, which exhibits similarities to the strong recent Arctic warming. For Greenland, the mid-Holocene provides the opportunity to investigate the processes, leading to this warming, in more detail and to potentially obtain new insights about the future development of the Arctic region (Yoshimori and Suzuki, 2019).

While General Circulation Models (GCMs) are generally able to reflect the direction and large-scale patterns of past climate  
45 changes (e.g. Timm and Timmermann, 2007; Smith and Gregory, 2012), they often fail to reproduce the magnitude of regional changes (Braconnot et al., 2012; Harrison et al., 2014), which are documented in various local climate archives. Thus, a scale gap might exist between the measured point information and the large-scale climate information generated by GCMs. The comparison of observational and GCM data can therefore be subject to considerable uncertainties (Felzer and Thompson, 2001).

Especially for structured landscapes, the spatial resolution in GCMs is often too coarse to resolve relevant local factors (Jost  
50 et al., 2005; Fischer and Jungclaus, 2011). Important properties like topography and surface conditions are consequently only represented in a generalized and imprecise form in climate simulations. In most cases, this does not meet the complex characteristics of the land surface and its associated interactions with the atmosphere. For stable water isotopes, key physical processes of isotope fractionation are therefore also often not entirely resolved in coarsely resolved GCMs, leading to  
55 differences between simulated and observational isotope data, especially in complex terrains (Sturm et al., 2005; Werner et al., 2011). Consequently, in many cases GCM results exhibit larger deviations to observational data than the results of corresponding Regional Climate Model (RCM) simulations (Sjolte et al., 2011; Russo and Cubasch, 2016; Ludwig et al., 2018).

In the presented study, isotope-enabled GCM simulation results for the Arctic region are dynamically downscaled with an  
60 isotope-enabled RCM to a higher temporal and spatial resolution. By means of such regional simulations, the spatial variability of the isotopic ratios in the Arctic is potentially increased, accounting for the heterogeneity of local conditions at the different ice core locations. In this way, the impact of highly resolved local conditions on the spatial variability of isotopic ratios is



investigated, and it is analysed, if such small-scale spatial variability can potentially explain the discrepancy between simulated and observed paleo-climate conditions in the Arctic region.

65 To explore this, the isotope-enabled version of the RCM COSMO-CLM (Rockel et al., 2008), COSMO\_iso (Pfahl et al., 2012; Christner et al., 2018), is used. The results of the standard variables from COSMO in the Arctic region under present-day conditions are evaluated in a separated study (Karremann et al., under preparation). In the scope of ERA-Interim reanalysis (Dee et al., 2011) driven simulations, the model showed that it is generally able to simulate reasonable near-surface temperatures and precipitation rates for Greenland and can therefore be used for isotope applications in this region. The

70 capability of COSMO\_iso to simulate realistic water isotopic ratios for Greenland is tested by downscaling a global present-day simulation with an isotope-enabled GCM for the Arctic region. The GCM and RCM results are subsequently compared to measured water isotope ratios from snow pit samples. Afterwards, the tested isotope-enabled COSMO\_iso model system is used to downscale an isotope-enabled GCM simulation for a mid-Holocene time-slice. The simulated isotopic ratios are evaluated against Greenland ice core data. Such a dynamical downscaling of global isotope simulations for Greenland under

75 mid-Holocene conditions, is performed for the first time in the framework of this study.

## 2 Methods

### 2.1 COSMO\_iso

#### 2.1.1 Model Description

80 In this study, simulated stable water isotope concentrations of HD<sup>16</sup>O and H<sub>2</sub><sup>18</sup>O with isotope-enabled GCMs (section 2.1.2), are regionally downscaled with COSMO\_iso (Pfahl et al., 2012), an isotope-enabled version of the numerical weather prediction model COSMO (Baldauf et al., 2011) (version 4.18). For the purpose of long-term climate simulations, isotope-routines of COSMO\_iso were implemented in COSMO-CLM (Rockel et al., 2008), the climate version of COSMO. In this context, the δD and δ<sup>18</sup>O ratios in the soil water and the surface layer snow are simulated with TERRA\_iso V.1 (Dütsch, 2017;

85 Christner et al., 2018), the isotope-enabled version of the multi-layer Land Surface Model TERRA-ML (Schrodin and Heise, 2001) in COSMO. In several studies, COSMO\_iso and TERRA\_iso were successfully employed for the simulation of isotopic ratios in the mid-latitudes (Pfahl et al., 2012; Aemisegger et al., 2015; Christner et al., 2018). In the presented study, the model system will be applied to the Arctic region. For this, some additional modifications regarding the treatment of snow and ice had to be implemented in the model:

90

#### **Snow albedo**

The surface albedo of snow is increased from 0.7 to 0.8 to improve the model agreement with measured values of short-wave reflectance and 2m temperature at stations from the Cooperative Institute for Research in Environmental Sciences at the University of Colorado Boulder (CIRES) in Central Greenland.



95

### **Snow layer thickness**

In the standard configuration of COSMO, the Greenland ice sheet is treated as a constant mass of ice, which is covered by a single snow layer. But in this model structure, dynamical processes within the ice sheet (flow, basal melt) are not included. As a result, the depth of the snow layer is constantly increasing and thus also its heat capacity. The model is therefore not able to reproduce the observed diurnal cycles of the 2m temperature at CIRES stations in Central Greenland. To avoid this spurious model behavior, the snow layer depth is limited to 5 cm in this study. Using this value, realistic diurnal cycles of the 2m temperature could be simulated.

### **Marine regions with sea ice cover**

To be able to simulate reasonable fractionation processes for marine regions with sea ice cover, a snow layer is also implemented on top of the sea ice (e.g., as suggested in Bonne et al., 2019). The isotopic composition of this surface snow layer is in this case set to the isotopic composition of the most recent precipitation.

### **Fractionation at snow covered surfaces**

Isotope fractionation during sublimation from a surface snow layer is poorly understood. Several different processes are suggested to be involved, which are not yet taken into account in the models, such as non-fractionating layer-by-layer sublimation, kinetic fractionation during sublimation into sub-saturated air, a diurnal cycle of sublimation combined with fractionating vapor deposition on the snow, and fractionating melt water sublimation combined with recrystallization of residual melt water have been suggested (see e.g. discussion in Christner et al., 2017). In this study, best agreement of simulation results with data of ground-based in situ measurements of near-surface water vapour at a site near Karlsruhe, Germany (measured with a Picarro water isotopologue analyser L2120-i), was found for the assumption of equilibrium fractionation during sublimation from surface layer snow and sea ice. However, the authors are aware that this description may only realistically approximate a much more complex interplay between different surface processes.

## **2.1.2 Model Simulation Setup**

In a first step, the capability of COSMO\_iso to realistically reflect the fractionating processes of stable water isotopes in Greenland is evaluated. For this, the nudged simulation outputs (standard and isotopic) from an isotope-enabled atmospheric model ECHAM5-wiso (Werner et al., 2011) simulation are dynamically downscaled with COSMO\_iso for the whole Arctic region. The data from the same ECHAM5-wiso simulation have been already used as boundary conditions for COSMO\_iso simulations over Europe by Christner et al. (2018). The simulation outputs from ECHAM5-wiso are at a T106 horizontal spatial resolution ( $1.1^\circ \times 1.1^\circ$ ) and on 31 atmospheric vertical levels. The dynamical fields were nudged every 6 hours towards ERA-Interim reanalysis data (Dee et al., 2011). The simulation period is 2008-2014. The spatial resolution of COSMO\_iso is



0.44° x 0.44°, corresponding to 50 km x 50 km in rotated coordinates (COSMO\_iso\_50km). Afterwards, the COSMO\_iso\_50km simulation is further downscaled to a spatial resolution of 0.0625° x 0.0625° (corresponding to about 7  
130 km x 7 km) for Greenland (COSMO\_iso\_7km). This high-resolution simulation covers only the year 2011, which was chosen for technical reasons. In the COSMO\_iso runs, the horizontal wind fields above the 850 hPa level are spectrally nudged (von Storch et al., 2000) towards the reanalysis-based dynamical fields of ECHAM5-wiso. This method ensures that consistent atmospheric boundary conditions build the framework for the fractionating processes simulated in COSMO\_iso.

The same model chain is applied to the mid-Holocene period. As no isotope-enabled ECHAM5-wiso simulation has been  
135 available for this period, atmospheric fields have been retrieved from a mid-Holocene simulation of the fully coupled model MPI-ESM-wiso (Cauquoin et al., 2019), whose atmospheric component is ECHAM6-wiso. The major ECHAM6 model changes compared to ECHAM5 include an improved representation of radiative transfer in the solar part of the spectrum, an improved representation of surface albedo, a new aerosol climatology and an improved representation of the middle atmosphere (Stevens et al., 2013). With COSMO\_iso, a representative time slice of 30 years is simulated for this climate  
140 period, only, since the regional COSMO\_iso simulations are computationally very expensive. The greenhouse gas concentrations and the orbital parameters are adapted, according to the Paleoclimate Modelling Intercomparison Project 4 experiment design (PMIP4, Kageyama et al., 2018). The model domain of the COSMO\_iso simulations is identical to the present-day simulations.

## 145 2.2 Observations

The capability of the isotope-enabled regional climate model COSMO\_iso to reproduce measured isotopic ratios in Greenland is evaluated by comparing the simulation results to different observational data. In this context, simulated  $\delta^{18}\text{O}$  ratios are compared to snow pit samples collected during the North Greenland Traverse (Fischer et al., 1998; Weißbach et al., 2016) and top core samples from four ice core locations (Renland (Vinther et al., 2008), Neem (Masson-Delmotte et al., 2015), GISP2  
150 (Grootes and Stuiver, 1997), Summit (Fischer, 2003)). The station numbers assigned to the respective samples within this study, as well as their locations and used  $\delta^{18}\text{O}$  values are summarized in Table 1. Since all snow pit samples cover different time periods, the present-day  $\delta^{18}\text{O}$  values (black numbers in Table 1) are calculated as an average of all available  $\delta^{18}\text{O}$  values measured between 1940 and 2007.

Ice core samples are also used to evaluate the simulated isotopic ratios for the mid-Holocene. Beside the already mentioned  
155 Renland and GISP2 samples, two more ice core samples, namely GRIP and NGRIP (Vinther et al., 2006), are used for the model evaluation. The mid-Holocene  $\delta^{18}\text{O}$  values (blue numbers in Table 1) are calculated as an average of the measured  $\delta^{18}\text{O}$  values in ice cores over the period 5.5 ka – 6.5 ka.



**Table 1:** Description of the observational data used in this study. The present-day  $\delta^{18}\text{O}$  values are calculated as an average of all available  $\delta^{18}\text{O}$  values measured in snow pit samples between 1940-2007. The mid-Holocene  $\delta^{18}\text{O}$  values are calculated as an average of the measured  $\delta^{18}\text{O}$  values in ice cores over the period 5.5 ka – 6.5 ka. Black numbers indicate present-day  $\delta^{18}\text{O}$  values, blue numbers mid-Holocene values.

165

No.	Name	Sample	Longitude	Latitude	$\delta^{18}\text{O}$	Reference
1	Renland	top core	-26.73	71.27	-27.38 (-26.44)	Vinther et al., 2008
2	NEEM	top core	-51.06	77.45	-33.24	Masson-Delmotte et al., 2015
3	GISP2	top core	-38.48	72.58	-34.95 (-34.83)	Grootes & Stuiver, 1997
4	Summit	top core	-37.64	73.03	-36.46	Fischer, 2003
5	B27_B28	snow pit	-46.48	76.65	-34.05	Weißbach et al., 2016
6	NGT03C93	snow pit	-37.62	73.94	-37.02	Weißbach et al., 2016
7	NGT06C93	snow pit	-37.62	75.25	-36.89	Weißbach et al., 2017
8	NGT14C93	snow pit	-36.4	76.61	-36.18	Weißbach et al., 2017
9	NGT23C94	snow pit	-36.5	78.83	-35.18	Weißbach et al., 2018
10	NGT27C94	snow pit	-41.13	80	-34.01	Weißbach et al., 2018
11	NGT30C94	snow pit	-45.91	79.34	-34.19	Weißbach et al., 2019
12	NGT33C94	snow pit	-44	78	-36.13	Weißbach et al., 2019
13	NGT37C95	snow pit	-49.21	77.25	-33.81	Weißbach et al., 2020
14	NGT39C95	snow pit	-46.48	76.65	-34.95	Weißbach et al., 2020
15	NGT42C95	snow pit	-43.49	76	-35.53	Weißbach et al., 2021
16	NGT45C95	snow pit	-42	75	-35.33	Weißbach et al., 2021
17	GRIP	top core	-37.64	72.58	-35.23 (-34.73)	Vinther et al., 2006
18	NGRIP	top core	-42.32	75.1	-35.15 (-34.69)	Vinther et al., 2006

### 3 Results

#### 3.1 Present-Day

170 Figure 1 shows the yearly mean  $\delta^{18}\text{O}$  values for the period 2008-2014 for Greenland, simulated with COSMO\_iso\_50km (a)  
 and ECHAM5-wiso (b). Additionally, the locations and the observed  $\delta^{18}\text{O}$  values of the 16 snow pit samples, used to assess  
 the models capability to reproduce observed  $\delta^{18}\text{O}$  ratios in Greenland, are illustrated.

In general, COSMO\_iso in a 50 km x 50 km spatial resolution is able to reflect the observed isotopic ratios at the 16 snow pit  
 samples and improves the simulation results of ECHAM5-wiso. In both simulations, the  $\delta^{18}\text{O}$  ratios are high near the coastline  
 175 and low in Central Greenland. But in COSMO\_iso\_50km, the  $\delta^{18}\text{O}$  ratios decline stronger from the coastline to the inland

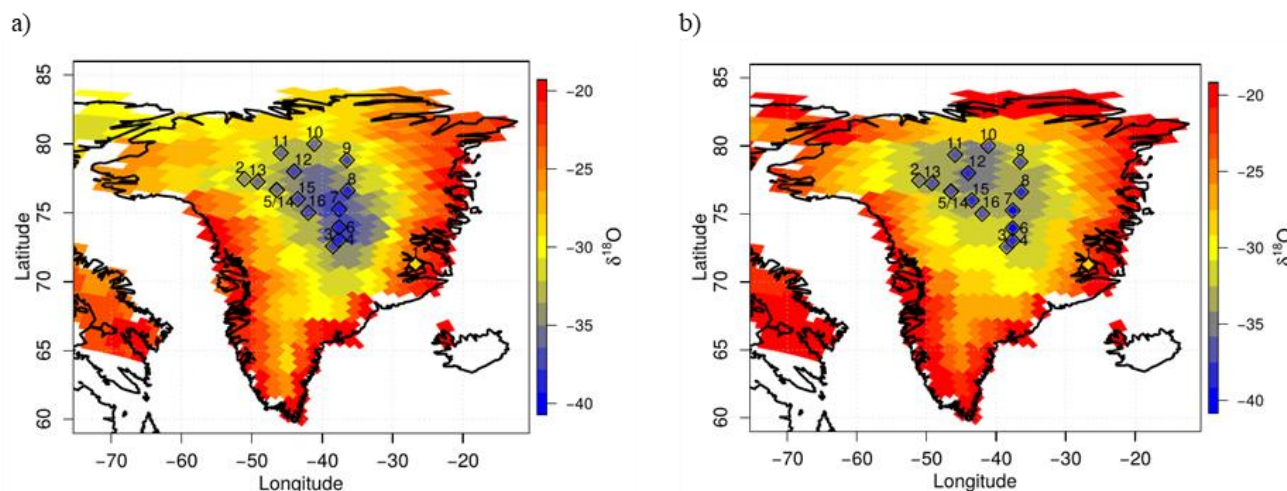


**Figure 1:** Yearly mean  $\delta^{18}\text{O}$  values of COSMO\_iso\_50km (a) and ECHAM5-wiso (b, interpolated to the COSMO\_iso\_50km grid) for the period 2008 - 2014 and the corresponding observations for the 16 snow pit samples (Table 1).

plateau than in ECHAM5-wiso. The spatial  $\delta^{18}\text{O}$  differences are consequently stronger pronounced and the general  
180 overestimation of  $\delta^{18}\text{O}$  ratios, which occurs in ECHAM5-wiso, is reduced in COSMO\_iso\_50km. Thus, the regional simulation  
reaches a better agreement with the observations. Especially for the snow pit samples at which ECHAM5-wiso exhibits strong  
deviations to the observed  $\delta^{18}\text{O}$  values (1,3,4,6,7,8,9,10,16; see Table 1), a regional downscaling with COSMO\_iso\_50km  
reduces the bias considerably (Figure 2). But for snow pit samples at which ECHAM5-wiso has already a high agreement with  
the observations (2,5,11,13,14), COSMO\_iso\_50km tends to increase the bias. A further downscaling with COSMO\_iso to a  
185 spatial resolution of 7 km x 7 km does not improve the simulation results anymore. The only exception constitutes the snow  
pit sample from Renland (1). Here, a considerable model bias in ECHAM5-wiso and COSMO\_iso\_50km is strongly reduced  
in COSMO\_iso\_7km.

The coastal area of Renland is characterized by a complex terrain and constitutes a special case for isotope-enabled modeling  
in Greenland. The snow pit sample is located in a transition zone from the homogeneous inland glaciation to the rugged  
190 coastline, where the glaciers calve into the sea. Thus, within short distances large differences in altitude and land surface  
characteristics occur in this region. The isotopic ratios in the snow pit sample are therefore strongly affected by these  
heterogeneous local conditions, which are insufficiently represented in the coarse model resolution of ECHAM5-wiso. By  
increasing the spatial resolution with regional climate modeling, also the representation of the associated small-scale processes  
is improved. This leads generally to a higher agreement of the simulation results with observations, as seen for the  
195 COSMO\_iso\_7km run for Renland (Figure 2).

However, an increase in spatial resolution is, especially in complex terrains, also associated with an enlarged heterogeneity of  
the surface characteristics and the related small-scale processes. This is because the GCM grid boxes are further divided in  
smaller RCM grid boxes and consequently higher as well as lower values (for e.g. altitude) are included within the same area.



In the case that a snow pit sample is located right at the border of two RCM grid boxes, the higher resolved model information  
200 does not necessarily have to match the local conditions in complex terrains. The characteristics of the adjacent RCM grid box  
might fit much better to the conditions of the snow pit sample. The differences between the model data and the observations  
can consequently get larger than for a coarser model resolution. Thus, in the following, snow pit samples are not anymore  
solely compared to the model grid boxes covering the samples location. Instead, it is investigated whether the  $\delta^{18}\text{O}$  range of  
all adjacent RCM grid boxes to a snow pit location is consistent with the observed  $\delta^{18}\text{O}$  value of the same site. For this, all  
205 RCM grid boxes located within the corresponding GCM grid box are included in the comparison with the observations.

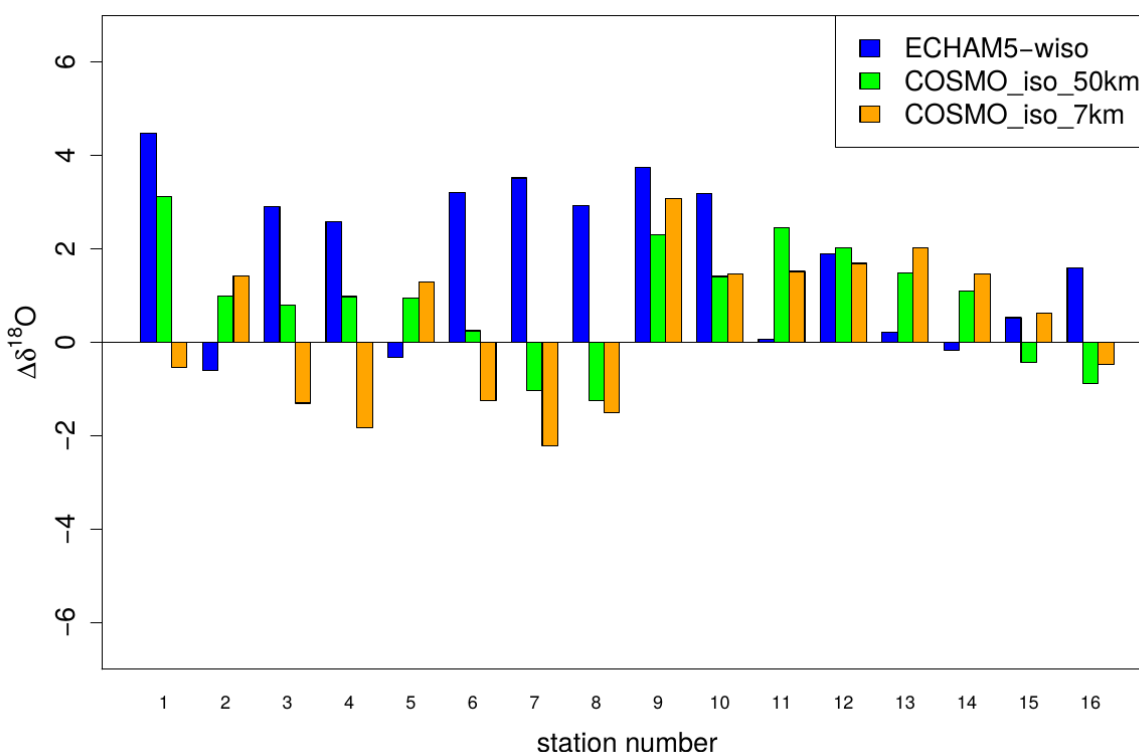


**Figure 2:** Differences ( $\Delta$ ) between simulated and observed  $\delta^{18}\text{O}$  values (model minus observation) for the model results of ECHAM5-wiso, COSMO\_iso\_50km, and COSMO\_iso\_7km, and snow pit samples / top core samples from ice cores from Greenland (simulation: 2011, observation: mean present values). Numbers refer to the different snow pit locations shown in Figure 1.

210

The spatial isotopic ratio variability of the COSMO\_iso\_50km grid boxes surrounding the 16 snow pit samples is shown as Box-Whiskers-plot in Figure 3a. The spatial isotopic ratio variability of the COSMO\_iso\_7km is shown in Figure 3b. In this spatial isotopic ratio variability, the  $\delta^{18}\text{O}$  values of all COSMO\_iso (50 km) and COSMO\_iso (7 km) grid boxes within the ECHAM5\_wiso grid box closest to the snow pit sample, are included. For 11 of the 16 snow pit samples  
215 (1,2,3,4,5,6,7,8,14,15,16) the range of the COSMO\_iso\_50km grid box variability is consistent with the observed  $\delta^{18}\text{O}$  values.



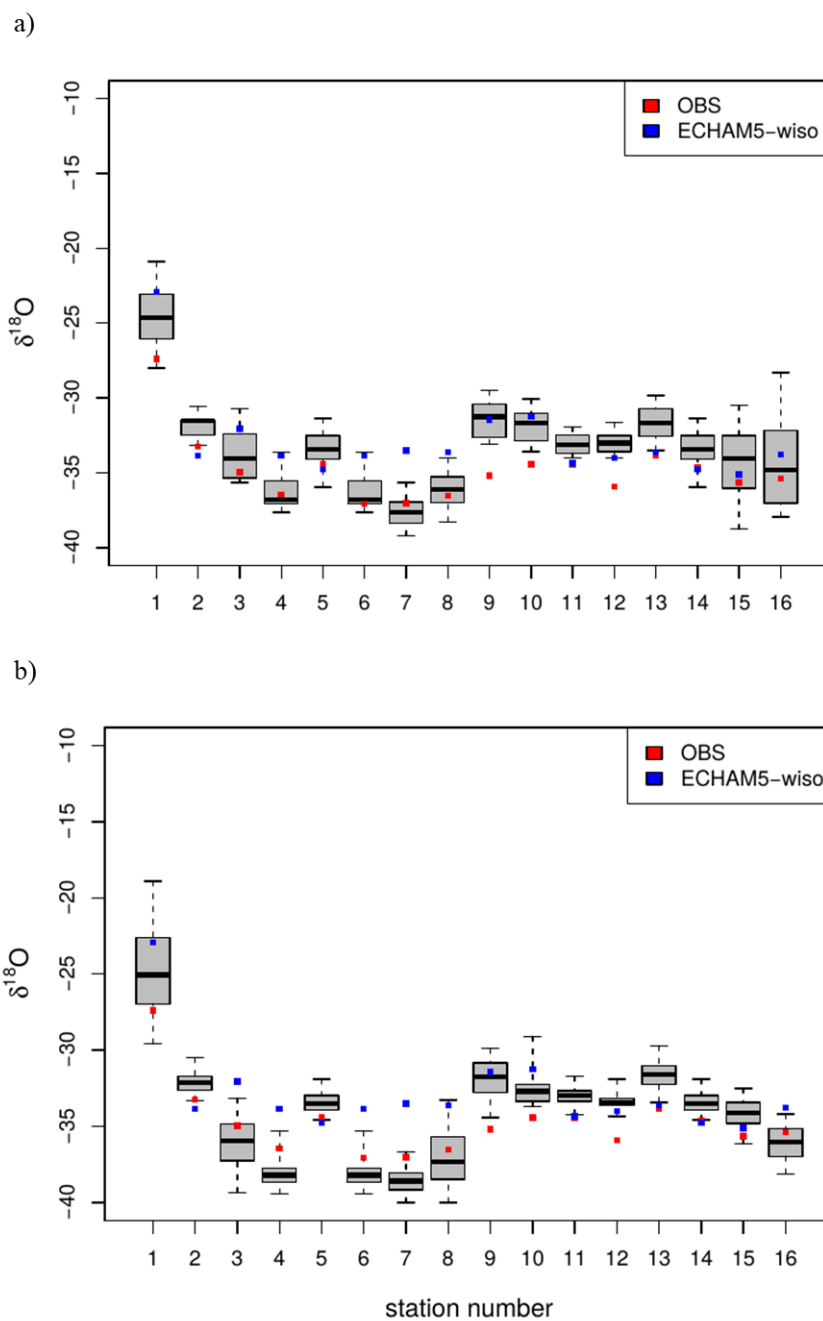


**Figure 3:** Present-day isotopic ratio variability of the COSMO\_iso grid boxes, surrounding the 16 snow pit samples for the (a) 50 km and (b) 7 km simulation. The black bar in the Box-Whiskers-plot represents the median of the isotope ratio distribution. The box comprises the upper and lower quartile, the whiskers the whole distribution. The ECHAM5-wiso results are shown by the blue dots and the observed  $\delta^{18}\text{O}$  values are shown by the red dots.



But for 5 of the 16 snow pit samples (9-13) the COSMO\_iso\_50km range of isotopic values does not fit with the observations. These stations are all located in the north of Greenland. In these latitudes, longitudes are converging and the differences in spatial resolution between ECHAM5-wiso and COSMO\_iso\_50km with its rotated pole become smaller. Thus, in the high latitudes less COSMO\_iso\_50km grid boxes are covered by one ECHAM5-wiso grid box, than in the south of Greenland. The spread of the COSMO\_iso\_50km results is consequently reduced and the COSMO\_iso\_50km  $\delta^{18}\text{O}$  range at these stations is not consistent anymore with the observed  $\delta^{18}\text{O}$  values.

A downscaling to 7 km does slightly increase the spread of the COSMO\_iso results. But still, the observed  $\delta^{18}\text{O}$  values from 5 of 16 snow pit samples are not covered within the modelled COSMO\_iso\_7km grid box variability (Figure 3b). Thus, a further downscaling to a spatial resolution of 7 km does not increase the accuracy of the simulated isotopic ratio spread within a ECHAM5-wiso grid box. In accordance with the missing benefits of the COSMO\_iso\_7km simulation and its increased computing time costs, only a COSMO\_iso\_50km simulation is performed for the mid-Holocene.

### 3.1 Mid-Holocene

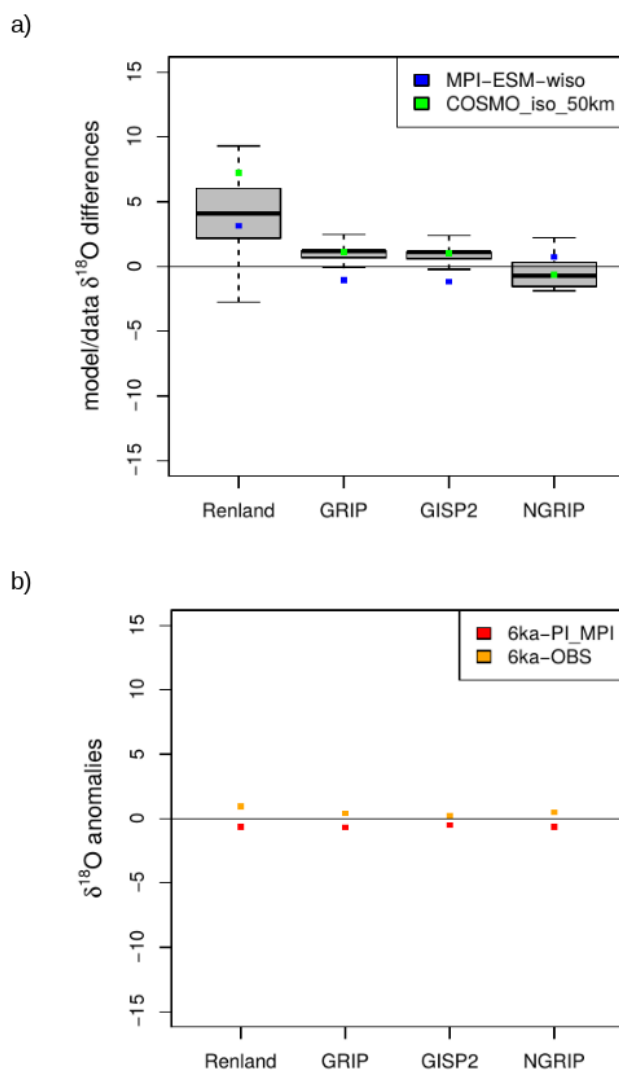
In Figure 4a the differences for the simulated MPI-ESM-wiso (blue) and COSMO\_iso\_50km (green) grid box results to the observed  $\delta^{18}\text{O}$  ratios at the corresponding ice cores are presented for the mid-Holocene. As in Figure 3, the spatial isotopic ratio variability of the COSMO\_iso\_50km grid boxes surrounding four Greenland ice core samples is shown as Box-Whiskers-plot. MPI-ESM-wiso properly reflects the isotopic ratios of the mid-Holocene from ice core data. For the inland ice cores (GRIP, GISP2, NGRIP), the simulated  $\delta^{18}\text{O}$  deviates only about 1 ‰ to the observations, at Renland the deviation is about 3 ‰. For GRIP and GISP2 the MPI-ESM-wiso simulations slightly underestimate the  $\delta^{18}\text{O}$  ratios, for NGRIP and Renland, the  $\delta^{18}\text{O}$  values are slightly overestimated.

In Figure 4b, the MPI-ESM-wiso model anomalies to the pre-industrial period (PI) conditions, which are based on a MPI-ESM-wiso PI-reference simulation performed by Cauquoin et al. (2019), are compared to the observed mid-Holocene-PI anomalies at the ice cores. The biases of the MPI-ESM-wiso mid-Holocene-PI model anomalies to the observed mid-Holocene-PI anomalies are for all ice cores very small. Overall, the mid-Holocene-PI model anomalies are at a similar level to the absolute mid-Holocene deviations. This finding shows that the good agreement of the MPI-ESM-wiso mid-Holocene absolute results with the ice core data is not achieved by chance. The good model performance in Greenland is rather caused by a realistically simulated mean climate state of the mid-Holocene. From a scientific perspective, therefore, the omission of a COSMO\_iso\_50km PI-reference simulation, for reasons of computing time, is justifiable.

COSMO\_iso\_50km simulates the opposite sign of MPI-ESM-wiso for the deviation of the  $\delta^{18}\text{O}$  values to the observations at the inland ice cores. That means that in GRIP and GISP2, the underestimated  $\delta^{18}\text{O}$  values in MPI-ESM-wiso are turned into overestimated  $\delta^{18}\text{O}$  values in COSMO\_iso\_50km, at NGRIP the overestimation is turned into an underestimation. But in contrast to the present-day simulations the net bias is not reduced. At Renland, again the bias is even increased. Thus, by just



255 looking at the absolute biases, the downscaling does not seem to bring an added value to the MPI-ESM-wiso results for mid-Holocene conditions. But taking also into account the isotopic ratio variability in the COSMO\_iso\_50km simulation, the model results are again in agreement with the isotopic ratios of the ice core samples.



260 **Figure 4:** (a) mid-Holocene isotopic ratio variability of the COSMO\_iso\_50km grid boxes surrounding four Greenland ice core samples. In each grid box, the simulated  $\delta^{18}\text{O}$  ratios are subtracted by the observed ratios in the ice cores. The black bar in the Box-Whiskers-plot represents the median of the isotope ratio distribution. The box comprises the upper and lower quartile, the whiskers the whole distribution. The MPI-ESM-wiso (blue dots) and COSMO\_iso\_50km (green dots) results for the grid boxes corresponding to the ice cores are also shown as differences to the observed  $\delta^{18}\text{O}$  ratios. (b) the anomalies of the MPI-ESM-wiso simulation to the PI conditions, based on a MPI-ESM-wiso PI-reference simulation (Cauquoin et al., 2019) are shown in red dots, the observed mid-Holocene-PI anomalies in orange dots.

265



The fact that, in contrast to the present-day simulations, only four observational data sets are available for the mid-Holocene, makes the assessment of the simulation results difficult. Moreover, the GRIP and GISP2 ice cores being located very close to each other (Figure 5), only three local isotope distributions clearly different from each other are available. Therefore in Figure 5a, the spatial isotopic ratio variability of the COSMO\_iso\_50km simulation is illustrated for whole Greenland. This spatial isotopic ratio variability is calculated as the standard deviation of all COSMO\_iso\_50km grid boxes within the respective MPI-ESM-wiso grid boxes. Figure 5a shows that at the coastline, the isotopic ratio variability of COSMO\_iso\_50km is considerably increased within the MPI-ESM-wiso grid boxes. In Central Greenland the increase in the isotopic ratio variability is lower. Thus, the simulated variability is high in regions where large orographic differences occur within short distances, like the coastal areas of Greenland, and lower for homogeneous terrain like the inland plateau. The Renland ice core is therefore located in an area of a high isotopic variability, the GRIP and GISP2 ice cores in an area of low isotopic variability. Nevertheless, regions with higher isotopic variability occur also in the inland plateau of Greenland. The NGRIP ice core, for instance, is located in an area of a moderate isotopic ratio variability. The four ice core drill sites are therefore located the three regions of Greenland with substantially different isotopic ratio variabilities.

The spatial surface temperature variability in the COSMO\_iso\_50km simulation, which is calculated in the same way as the isotopic ratio variability, is shown in Figure 5b. Near the coastline, the surface temperature variability is high, highlighting how important the land surface characteristics are for the regional temperature variability. But in Central Greenland almost no variability occurs. This is in contrast to the water isotope ratio, exhibiting also regional variations over the inland plateau (Figure 5a). The spatial distribution of  $\delta^{18}\text{O}$  does consequently not only depend on land surface processes, but also on dynamic atmospheric processes. In this way, isotopic ratios based on atmospheric fractionation processes along the trajectory of an air mass, are transported to Central Greenland and increase there the isotopic variability.

The same pattern occurs for the spatial isotope-temperature gradient (Figure 6a), representing the relation between the surface temperatures and the  $\delta^{18}\text{O}$  values. The spatial gradient is thereby calculated between the simulated  $\delta^{18}\text{O}$  ratios and surface temperatures at all COSMO\_iso\_50km grid boxes within the respective MPI-ESM-wiso grid boxes. At the coastline, the  $\delta^{18}\text{O}$ -temperature gradient is low, reflecting the high surface temperature and  $\delta^{18}\text{O}$  variability in this region. In Central Greenland the gradient is high, which is the result of the low surface temperature variability and the simultaneously increased  $\delta^{18}\text{O}$  variability. This pattern does not only apply for the mid-Holocene, but also for the present-day COSMO\_iso\_50km simulation (Figure 6b). In the present-day simulation the contrast between the coastal regions and the inland plateau is even more clearly pronounced. The spatial variabilities of the surface temperature and the  $\delta^{18}\text{O}$  ratio in the mid-Holocene follow consequently the same mechanisms as for present-day.

295



300

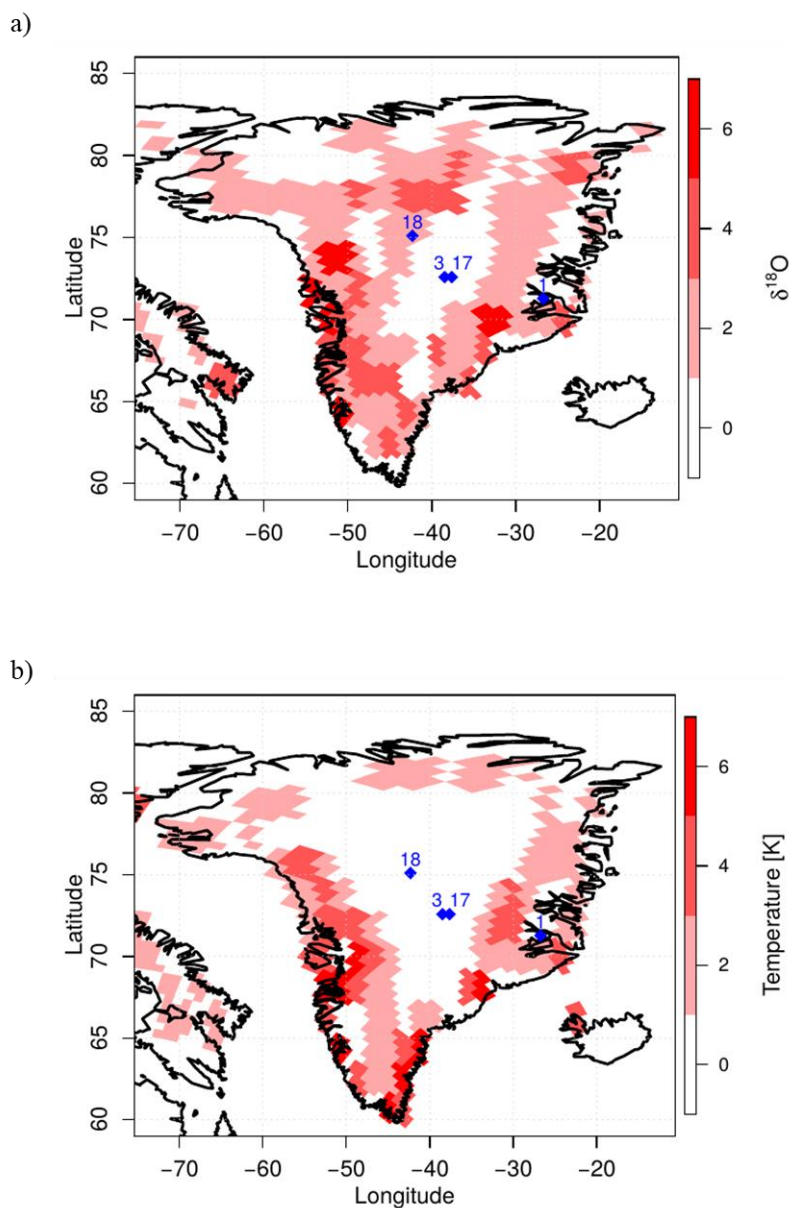
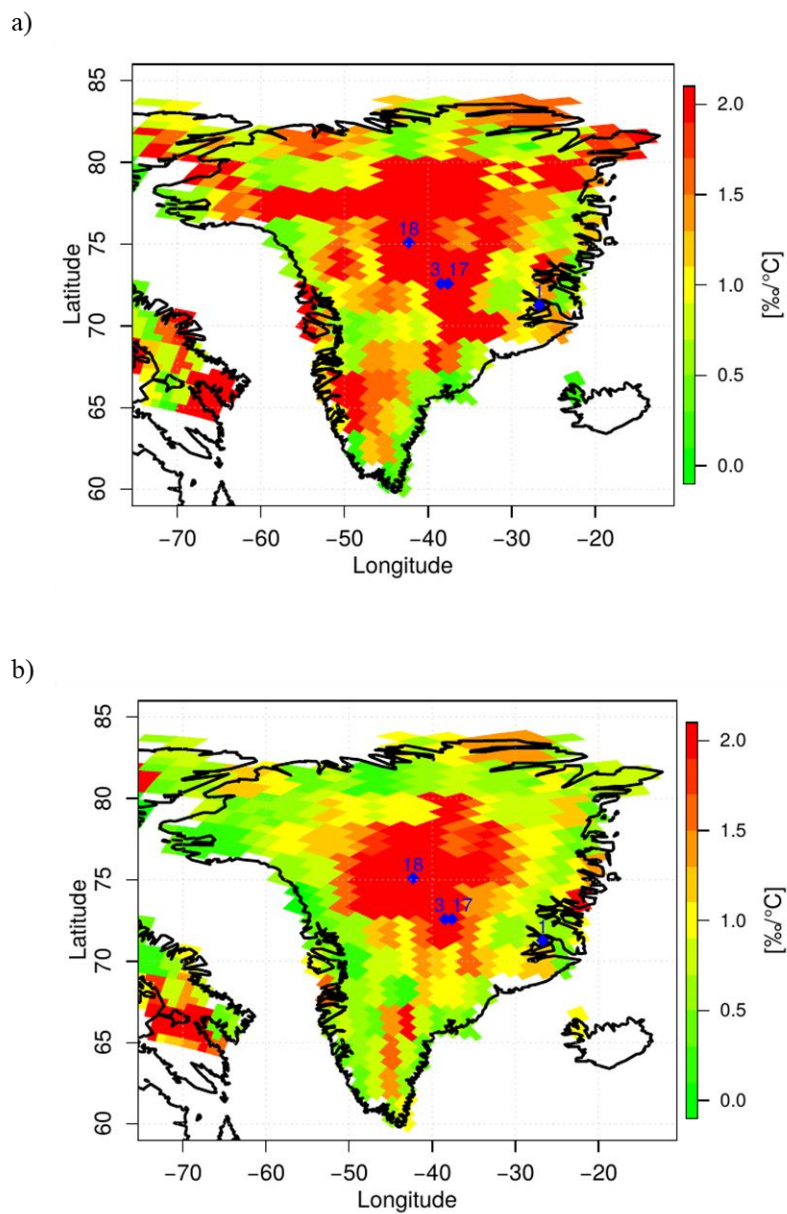


**Figure 5:** Simulated variability (calculated as standard deviation) in the mid-Holocene, for (a) the isotopic ratio and (b) the surface temperature, derived from the COSMO\_iso\_50km grid boxes within the respective MPI-ESM-wiso grid boxes for whole Greenland. The locations of the ice core samples are shown in blue.



305 **Figure 6:** Spatial  $\delta^{18}\text{O}$ -temperature gradient for Greenland, calculated between the simulated  $\delta^{18}\text{O}$  ratios and surface temperatures at all COSMO\_iso\_50km grid boxes within the respective grid boxes of (a) MPI-ESM-wiso for the mid-Holocene simulation and (b) ECHAM5-wiso for the present-day simulation. The locations of the ice core samples are shown in blue.



#### 310 4 Discussion and Conclusions

The results of several global paleo-climate simulations exhibit considerable deviations to the observed regional climate patterns during the Holocene (Braconnot et al., 2012). In the presented study, for the first time, regional climate simulations with an isotope-enabled RCM are performed for Greenland to potentially improve the agreement to climate observations in this region for the mid-Holocene. In a first step, the capability of the isotope-enabled RCM COSMO\_iso to reproduce observed isotopic ratios for Greenland is demonstrated.

The COSMO\_iso simulation results show that a spatial resolution of 50 km already leads to reasonable  $\delta^{18}\text{O}$  values. Especially in regions where the global ECHAM5-wiso model, which has been used to derive necessary forcing fields for the COSMO\_iso simulations, deviates strongly from the observed  $\delta^{18}\text{O}$  values, the bias is considerably reduced by the regional climate simulation with COSMO\_iso. In complex terrain like the coastal areas of Greenland, the results can be further improved with an additional downscaling to a spatial resolution of 7 km. In such simulations with high spatial resolution, small-scale processes are described in more detail (e.g. Torma et al., 2015; Coppola et al., 2018) and thus the local characteristics at ice core sites are better taken into account (Sturm et al., 2005; Werner et al., 2011). But for northern Greenland, regional climate simulations with COSMO\_iso even increase the deviations to the observations and the local COSMO\_iso  $\delta^{18}\text{O}$  variability at the ice core drill sites is not consistent with the observed  $\delta^{18}\text{O}$  values. In this region, the gain in resolution is small for a downscaling and consequently the simulation results are not improved. But all in all, the results show that COSMO\_iso is able to provide reasonable isotopic ratios for Greenland and thus, can be applied for paleo-climate simulations.

For the mid-Holocene, MPI-ESM-wiso is in good agreement with observed ice core data in Greenland, as already described by Cauquoin et al. (2019). The model bias is, in this context, not further reduced by a downscaling with COSMO\_iso. But an increase in the spatial model resolution leads also to an increase in the models degrees of freedom. This in turn can lead, in the case of an already good performance of the driving model, to additional noise and thus, a deviating RCM behavior with even an increase in the absolute model bias, as seen for the mid-Holocene and the present-day simulations in Central Greenland.

Another consequence of these increased degrees of freedom in the COSMO\_iso simulation is that the spatial variability of the simulated  $\delta^{18}\text{O}$  ratios is enhanced. Therefore, by analyzing the spatial variability of the COSMO\_iso results, it can be demonstrated that most of the observed  $\delta^{18}\text{O}$  values lie within a range of spatially varying  $\delta^{18}\text{O}$  values, which can be derived in a physically consistent way by a regional downscaling of the spatially coarse MPI-ESM-wiso model results. This applies for both, the present-day runs and the regional paleo-climate simulations for the mid-Holocene in Greenland. The deviation between the coarser resolved MPI-ESM-wiso results and the finer resolved observations is therefore potentially caused by the missing representation of important small-scale processes, which are induced by e.g. the surface conditions or orographic effects over Greenland.

As  $\delta^{18}\text{O}$  ratios are used as an indicator for temperatures in past climates (Dansgaard et al., 1969; Masson-Delmotte et al., 2005; Jouzel, 2013), it is important to understand how the presented COSMO\_iso simulations might be able to improve these isotope-based temperatures reconstructions. In general, the regional surface temperature variability and the regional  $\delta^{18}\text{O}$  variability



show similar patterns for Greenland. In both cases the variability is high at the coast and low on the inland plateau. The same patterns as in the mid-Holocene can also be seen for the present-day simulations. In this context, the simulated spatial  $\delta^{18}\text{O}$ -  
345 temperature gradient reflects the same patterns as simulated by Sjolte et al. (2011) under present-day conditions for Greenland. This spatial variability patterns indicate that the regional surface temperature variability highly depends on the surface characteristics. However, for the regional isotopic ratio variability, this dependence appears to be less pronounced. At the coastline, a clear relationship between surface temperatures and measured  $\delta^{18}\text{O}$  ratios in ice cores can be derived, while in Central Greenland this relation is less pronounced. These spatial differences might be explained by the fact that isotope changes  
350 are an integrated signal of the meso-scale variability of atmospheric processes (Dansgaard, 1964; Merlivat and Jouzel, 1979; Gat, 1996), which might partially be decoupled from surface temperature changes in homogeneous terrain.

The presented study demonstrates that the isotope-enabled MPI-ESM-wiso - COSMO\_iso model chain with realistically implemented stable water isotope fractionation processes constitutes a useful supplement to reconstruct regional paleo-climate conditions during the mid-Holocene in Greenland. This approach might also be very helpful for other isotope-enabled GCMs  
355 and their deviations to observed isotope ratios in different paleo-time periods and regions. Particularly in regions, in which large differences occur between simulated and observed  $\delta^{18}\text{O}$  ratios, like Europe and North America (Cauquoin et al., 2019; Comas-Bru et al., 2019), an improved representation of small-scale processes can potentially reduce these biases, and consequently, the reconstruction of regional paleo-climate patterns can become more reliable. To prove this hypothesis, in follow-up studies, more time slices will be simulated with the presented MPI-ESM-wiso – COSMO\_iso model chain for  
360 different periods and different regions.

365 *Code availability.* The isotope-enabled version COSMO\_iso is available upon request from Marcus Breil. The isotopic version MPI-ESM-wiso is available upon request on the AWI's FusionForge repository (<https://swrepo1.awi.de/projects/mpe-esm-wiso/>).

370 *Author contributions.* MB performed the COSMO\_iso mid-Holocene simulations, EC the COSMO\_iso present-day simulation. The ECHAM5-wiso simulations were performed by MW, the MPI-ESM-wiso simulations by AC. MB analysed the presented model results and wrote the manuscript with contributions from all co-authors.

375 *Competing interests.* The authors declare that they have no conflict of interest.





*Acknowledgements.* This work was supported by the German Federal Ministry of Education and Research (BMBF) as a Research for Sustainability initiative (FONA) through PalMod project (FKZ: 01LP1511B). All simulations were performed at  
380 the German Climate Computing Center (DKRZ).

## References

- Aemisegger, F., J. K. Spiegel, S. Pfahl, H. Sodemann, W. Eugster, and H. Wernli: Isotope meteorology of cold front passages: A case study combining observations and modeling, *Geophysical Research Letters*, 42(13), 5652–5660,  
385 doi:10.1002/2015GL063988, 2015.
- Baldauf M, Seifert A, Förstner J, Majewski D, Raschendorfer M: Operational convective-scale numerical weather prediction with the COSMO model: description and sensitivities. *Mon Weather Rev*, 139:3887–3905, 2011.
- Bonne, J. L., and Coauthors: Resolving the controls of water vapour isotopes in the Atlantic sector. *Nature communications*, 10(1), 1632, 2019.
- 390 Braconnot, P., and Coauthors: Evaluation of climate models using palaeoclimatic data. *Nature Climate Change*, 2(6), 417, 2012.
- Cauquoin, A., Werner, M. and Lohmann, G.: Water isotopes – climate relationships for the mid-Holocene and pre-industrial period simulated with an isotope-enabled version of MPI-ESM, *Clim. Past*, 15, 1913-1937, doi:10.5194/cp-15-1913-2019, 2019.
- 395 Comas-Bru, L., Harrison, S. P., Werner, M., Rehfeld, K., Scroton, N., Veiga-Pires, C., and SISAL working group members: Evaluating model outputs using integrated global speleothem records of climate change since the last glacial, *Clim. Past*, 15, 1557–1579, <https://doi.org/10.5194/cp-15-1557-2019>, 2019.
- Coppola, E., and Coauthors: A first-of-its-kind multi-model convection permitting ensemble for investigating convective phenomena over Europe and the Mediterranean. *Climate Dynamics*, 1-32, 2018.
- 400 Craig, H., and Gordon, L. I.: Deuterium and oxygen 18 variations in the ocean and marine atmosphere, Stable isotopes in oceanographic studies and paleotemperatures, 23. Pisa, Italy: Conoglio Nazionale delle Ricerche, Laboratorio di Geologia Nucleare, 1965.
- Christner, E., M. Kohler, and M. Schneider: The influence of snow sublimation and meltwater evaporation on  $\delta D$  of water vapor in the atmospheric boundary layer of central Europe, *Atmospheric Chemistry and Physics*, 17(2), 1207–1225,  
405 doi:10.5194/acp-17-1207-2017, 2017.
- Christner, E., and Coauthors: The climatological impacts of continental surface evaporation, rainout, and subcloud processes on  $\delta D$  of water vapor and precipitation in Europe. *Journal of Geophysical Research: Atmospheres*, 123(8), 4390-4409, 2018.



- Dansgaard, W.: The abundance of O18 in atmospheric water and water vapour. *Tellus*, 5(4), 461-469, 1953.
- Dansgaard, W.: Stable isotopes in precipitation. *Tellus*, 16(4), 436-468, 1964.
- 410 Dansgaard, W., Johnsen, S. J., Møller, J., and Langway, C. C.: One thousand centuries of climatic record from Camp Century on the Greenland ice sheet. *Science*, 166(3903), 377-380, 1969.
- Dee, D. P., and Coauthors: The ERA-Interim reanalysis: Configuration and performance of the data assimilation system. *Quarterly Journal of the royal meteorological society*, 137(656), 553-597, 2011.
- Dütsch, M.: Stable water isotope fractionation processes in weather systems and their influence on isotopic variability on  
415 different time scales. Diss no. 23939, Ph.D. thesis, ETH Zurich, 2017.
- Felzer, B., and Thompson, S. L.: Evaluation of a regional climate model for paleoclimate applications in the Arctic. *Journal of Geophysical Research: Atmospheres*, 106(D21), 27407-27424, 2001.
- Fischer, H., and Coauthors: Little ice age clearly recorded in northern Greenland ice cores. *Geophysical Research Letters*, 25(10), 1749-1752, 1998.
- 420 Fischer, H.: Stable oxygen isotopes on snow pit ngt01C93 from the North Greenland Traverse. doi:10.1594/PANGAEA.133399, 2003.
- Fischer, N., and Jungclaus, J. H.: Evolution of the seasonal temperature cycle in a transient Holocene simulation: orbital forcing and sea-ice. *Climate of the Past*, 7, 1139-1148, 2011.
- Gat, J. R.: Oxygen and hydrogen isotopes in the hydrological cycle. *Annual Review of Earth and Planetary Sciences*, 24(1),  
425 225–262. <https://doi.org/10.1146/annurev.earth.24.1.225>, 1996.
- Grootes, P. M., and Stuiver, M.: Oxygen 18/16 variability in Greenland snow and ice with 10– 3- to 105-year time resolution. *Journal of Geophysical Research: Oceans*, 102(C12), 26455-26470, 1997.
- Harrison, S. P., and Coauthors: Climate model benchmarking with glacial and mid-Holocene climates. *Climate Dynamics*, 43(3-4), 671-688, 2014.
- 430 Jost, A., Lunt, D., Kageyama, M., Abe-Ouchi, A., Peyron, O., Valdes, P. J., and Ramstein, G.: High-resolution simulations of the last glacial maximum climate over Europe: a solution to discrepancies with continental palaeoclimatic reconstructions?. *Climate Dynamics*, 24(6), 577-590, 2005.
- Jouzel, J., and Merlivat, L.: Deuterium and oxygen 18 in precipitation: Modeling of the isotopic effects during snow formation. *Journal of Geophysical Research: Atmospheres*, 89(D7), 11749-11757, 1984.
- 435 Jouzel, J.: A brief history of ice core science over the last 50 yr, *Clim. Past*, 9, 2525–2547, 2013.
- Kageyama, M., and Coauthors: The PMIP4 contribution to CMIP6–Part 1: Overview and over-arching analysis plan, *Geosci. Model Dev.*, 11, 1033–1057, 2018.
- Karremann, M.K., and Schädler, G.: Parametrisation of variables having an impact on the Greenland surface mass balance using regional climate model simulations, to be submitted to Atmosphere.
- 440 Ludwig, P., Gómez-Navarro, J. J., Pinto, J. G., Raible, C. C., Wagner, S., and Zorita, E.: Perspectives of regional paleoclimate modeling. *Annals of the New York Academy of Sciences*, 2018.



- Marcott, S. A., Shakun, J. D., Clark, P. U., and Mix, A. C.: A reconstruction of regional and global temperature for the past 11,300 years. *Science*, 339(6124), 1198-1201, 2013.
- 445 Masson-Delmotte, V., and Coauthors: GRIP deuterium excess reveals rapid and orbital-scale changes in Greenland moisture origin. *Science*, 309(5731), 118-121, 2005.
- Masson-Delmotte, V., and Coauthors: Recent changes in north-west Greenland climate documented by NEEM shallow ice core data and simulations, and implications for past-temperature reconstructions. *The Cryosphere Discussions*, Copernicus, 2015, pp.1481-1504. 10.5194/tc-9-1481-2015, 2015.
- 450 Merlivat, L., and Jouzel, J.: Global climatic interpretation of the deuterium-oxygen 18 relationship for precipitation. *Journal of Geophysical Research: Oceans*, 84(C8), 5029-5033, 1979.
- Moossen, H., Bendle, J., Seki, O., Quillmann, U., and Kawamura, K.: North Atlantic Holocene climate evolution recorded by high-resolution terrestrial and marine biomarker records. *Quaternary Science Reviews*, 129, 111-127, 2015.
- Pfahl, S., Wernli, H., and Yoshimura, K.: The isotopic composition of precipitation from a winter storm—a case study with the limited-area model COSMOiso. *Atmos. Chem. Phys*, 12(3), 1629-1648, 2012.
- 455 Rockel, B., Will, A., and Hense, A.: The regional climate model COSMO-CLM (CCLM). *Meteorologische Zeitschrift*, 17(4), 347-348, 2008.
- Russo, E. and Cubasch, U.: Mid-to-late Holocene temperature evolution and atmospheric dynamics over Europe in regional model simulations. *Clim. Past* 12: 1645–1662, 2016.
- Schrodin, R., and E. Heise: The multi-layer version of the DWD soil model TERRA-LM, Consortium for Small-Scale  
460 Modelling (COSMO) Tech. Rep., 2, 16, 2001.
- Sjolte, J., Hoffmann, G., Johnsen, S. J., Vinther, B. M., Masson-Delmotte, V., and Sturm, C.: Modeling the water isotopes in Greenland precipitation 1959–2001 with the meso-scale model REMO-iso. *Journal of Geophysical Research: Atmospheres*, 116(D18), 2011.
- Smith, R. S., and Gregory, J.: The last glacial cycle: transient simulations with an AOGCM. *Climate dynamics*, 38(7-8), 1545-  
465 1559, 2012.
- Stevens, B., and Coauthors: Atmospheric component of the MPI-M earth system model: ECHAM6. *Journal of Advances in Modeling Earth Systems*, 5(2), 146-172, 2013.
- Sturm, K., Hoffmann, G., Langmann, B., and Stichler, W.: Simulation of  $\delta^{18}\text{O}$  in precipitation by the regional circulation model REMOiso. *Hydrological Processes: An International Journal*, 19(17), 3425-3444, 2005.
- 470 Timm, O., and Timmermann, A.: Simulation of the last 21 000 years using accelerated transient boundary conditions. *Journal of Climate*, 20(17), 4377-4401, 2007.
- Torma, C., Giorgi, F., and Coppola, E.: Added value of regional climate modeling over areas characterized by complex terrain—Precipitation over the Alps. *Journal of Geophysical Research: Atmospheres*, 120(9), 3957-3972, 2015.
- Vinther, B. M., and Coauthors: A synchronized dating of three Greenland ice cores throughout the Holocene. *Journal of  
475 Geophysical Research: Atmospheres*, 111(D13), 2006.



- Vinther, B. M., and Coauthors: Synchronizing ice cores from the Renland and Agassiz ice caps to the Greenland Ice Core Chronology. *Journal of Geophysical Research: Atmospheres*, 113(D8), 2008.
- von Storch, H., H. Langenberg, and F. Feser: A Spectral Nudging Technique for Dynamical Downscaling Purposes, *Monthly Weather Review*, 128(10), 3664–3673, doi:10.1175/1520-0493(2000)128;3664:ASNTFD;2.0.CO;2, 2000.
- 480 Weißbach, S., A. Wegner, T. Opel, H. Oerter, B. M. Vinther, and S. Kipfstuhl: Accumulation rate and stable oxygen isotope ratios of the ice cores from the North Greenland Traverse, doi:10.1594/PANGAEA.849161, 2016.
- Yoshimori, M., and Suzuki, M.: The relevance of mid-Holocene Arctic warming to the future. *Climate of the Past*, 15(4), 1375-1394, 2019.